

Research Article

MAP Channel-Estimation-Based PIC Receiver for Downlink MC-CDMA Systems

Hakan Doğan,¹ Erdal Panayırçı,² Hakan A. Çırpan,¹ and Bernard H. Fleury³

¹ Department of Electrical and Electronics Engineering, Istanbul University, Avcılar 34850, Istanbul, Turkey

² Department of Electronics Engineering, Kadir Has University, Cibali 34083, Istanbul, Turkey

³ Section Navigation and Communications, Department of Electronic Systems, Aalborg University Fredrik Bajers Vej 7A3 DK-9000 Aalborg, Denmark and The Telecommunications Research Center, Donau City Strasse 1, 1220 Vienna (ftw.), Austria

Correspondence should be addressed to Hakan Doğan, hdogan@istanbul.edu.tr

Received 15 May 2007; Revised 10 September 2007; Accepted 2 October 2007

Recommended by Arne Svensson

We propose a joint MAP channel estimation and data detection technique based on the expectation maximization (EM) method with parallel interference cancellation (PIC) for downlink multicarrier (MC) code division multiple access (CDMA) systems in the presence of frequency selective channels. The quality of multiple access interference (MAI), which can be improved by using channel estimation and data estimation of all active users, affects considerably the performance of PIC detector. Therefore, data and channel estimation performance obtained in the initial stage has a significant relationship with the performance of PIC. So obviously it is necessary to make excellent joint data and channel estimation for initialization of PIC detector. The EM algorithm derived estimates the complex channel parameters of each subcarrier iteratively and generates the soft information representing the data a posterior probabilities. The soft information is then employed in a PIC module to detect the symbols efficiently. Moreover, the MAP-EM approach considers the channel variations as random processes and applies the Karhunen-Loeve (KL) orthogonal series expansion. The performance of the proposed approach is studied in terms of bit-error rate (BER) and mean square error (MSE). Throughout the simulations, extensive comparisons with previous works in literature are performed, showing that the new scheme can offer superior performance.

Copyright © 2008 Hakan Doğan et al. This is an open access article distributed under the Creative Commons Attribution License, which permits unrestricted use, distribution, and reproduction in any medium, provided the original work is properly cited.

1. INTRODUCTION

Traditional wireless technologies are confronted with new challenges in meeting the ubiquity and mobility requirements of cellular systems. Extensive attempts have therefore been made in recent years to provide promising avenue that makes efficient utilization of the limited bandwidth and cope with the adverse access environments. These include the development of several modulation and multiple access techniques. Among these, multicarrier (MC) and code division multiple access (CDMA) have gained considerable interest due to their considerable performance [1, 2].

MC modulation technique, known also as OFDM (orthogonal frequency division multiplexing), has emerged as an attractive and powerful alternative to conventional modulation schemes in the recent past due to its various advantages. The advantages of MC which lie behind such a success are robustness in the case of multipath fading, a very reduced

system complexity due to equalization in the frequency domain and the capability of narrow-band interference rejection. OFDM has already been chosen as the transmission method for the European radio (DAB) and TV (DVB-T) standard and is used in xDSL systems as well. Supporting multiple users can be achieved in a variety of ways. One popular multiple access scheme is CDMA. CDMA makes use of spread spectrum modulation and distinct spreading codes to separate different users using the same channel. It is well known that CDMA system has an ability to reduce user's signal power during transmission using a spreading so that the user can communicate with a low-level transmitted signal closed to noise power level. As a combination of MC and CDMA techniques, it combines the advantages of both MC and CDMA [1–3].

To evaluate the performance of these systems, ideal knowledge of transmission parameters is often assumed known. Iterative receivers for coded MC-CDMA promise

a significant performance gain compared to conventional noniterative receivers by using combined minimum mean square error-parallel interference cancellation (combined MMSE-PIC) detector [5] assuming perfectly known channel impulse response. However, the performance of MC-CDMA-based transmission systems under realistic conditions critically depends on good estimate of the parameters, such as the channel parameters. In [4], different detection schemes were considered for least square estimation case as well as perfect channel case.

The quality of multiple access interference (MAI), which can be improved by using channel estimation and data estimation of all active users, affects considerably the performance of PIC detector. Therefore, data and channel estimation performance is obtained in the initial stage has a significant relationship with the performance of PIC. So obviously it is necessary to make excellent joint data and channel estimation for initialization of PIC detector. Inspired by the conclusions in [4, 5], including channel estimation into the iterative receiver yields further improvements. We therefore consider iterative channel estimation techniques based on the expectation-maximization (EM) algorithm in this paper.

The EM algorithm is a broadly applicable approach to the iterative computation of parameters from intractable and high complexity likelihood functions. An EM approach proposed for the general estimation from superimposed signals [6] is applied to the channel estimation for OFDM systems and compared with SAGE version in [7]. For CDMA systems, Nelson and Poor [8] extend the EM and SAGE algorithms for detection, rather than for estimation of continuous parameters. Moreover, EM-based channel estimation algorithms were investigated in [9, 10] for synchronous uplink DS-SS-CDMA and asynchronous uplink DS-SS-CDMA systems, respectively. Unlike the EM approaches, we adopt a two-step detection procedure: (i) use the EM algorithm to estimate the channel (frequency domain estimation) and (ii) use the estimated channel to perform coherent detection [11, 12]. The paper has several major novelties and contributions. The major contribution of the paper is to obtain EM-based channel estimation algorithm approach as opposed to the existing works in the literature which mostly assumed that the data is known at the receiver through a training sequence. Note that very small number of pilots used in our approach is necessary only for initialization of the EM algorithm leading to channel estimation. Although, the joint data and channel estimation technique with EM algorithm seems to be attractive in practice, it is known that the convergency of the algorithm is much slower, it is more sensitive to the initial selection of the parameters and the algorithm is more computationally complex than the techniques that deal with only channel estimation. As it is known in the estimation literature, non-data-aided estimation techniques are more challenging mainly due to a data-averaging process which must be performed prior to optimization step. The proposed EM-MAP receiver compared with the combined MMSE-PIC receiver in the case of LS, LMMSE, and perfect channel estimation [4].

Another significant contribution of the paper comes from the fact that the proposed approach considers the

channel variations as random processes and applies the Karhunen-Loeve (KL) orthogonal series expansion. It was shown that KL expansion enable us to estimate the channel in a very simple way without taking inverse of large-dimensional matrices for OFDM system [11, 12]. However, this property will not help to avoid matrix inversion for the signal model in this paper as shown in Section 4. On the other hand, we show that optimal truncation property of the KL expansion help to decrease inverse matrix dimension so that reduction in computational load on the channel estimation algorithm can be done.

The rest of this paper is organized as follows. In Sections 2 and 3 we introduce the model of a downlink MC-CDMA system and the corresponding channel model established, respectively. Using the discrete-time model, the maximum a posteriori (MAP) channel estimation algorithm is derived in Section 4. Moreover, in this section, truncation property of the KL expansion and complexity calculation of the proposed algorithm are also given. In the next section, PIC-detection scheme is then developed for the proposed channel estimation algorithm. Finally, computer simulation results are presented with detailed discussions in Section 6, and conclusions are drawn in Section 7.

Notation: Vectors (matrices) are denoted by boldface lower (upper) case letters; all vectors are column vectors; $(\cdot)^T$, $(\cdot)^\dagger$ and $(\cdot)^{-1}$ denote the transpose, conjugate transpose, and matrix inversion, respectively; \mathbf{I}_L denotes the $L \times L$ identity matrix; $\text{diag}\{\cdot\}$ denotes a diagonal matrix.

2. DOWNLINK MC-CDMA

Transmission of MC-CDMA signals from the base station to mobile stations forms the downlink transmission. The Base station must detect all the signals while each mobile is related with its own signal. In the downlink applications, all the signals arriving from the base station to specific user propagate through the same channel. Therefore, channel estimation methods that is developed for OFDM systems can be applicable for downlink application of MC-CDMA systems [11].

Let b^k 's denote the QPSK modulated symbols that would be send for k th user within mobile cell $k = 1, \dots, K$ where K is the number of mobile users which are simultaneously active. The base station spread the data b^k 's over chips of length N_c by means of specific orthogonal spreading sequences, $\mathbf{c}^k = (c_1^k, c_2^k, \dots, c_{N_c}^k)^T$ where each chip, c_i^k , takes values in the set $\{-1/\sqrt{N_c}, 1/\sqrt{N_c}\}$. Then, the spreaded sequences of all users $\mathbf{c}^k b^k$ are summed together to form the input sequences of the OFDM block. After summation process, OFDM modulator block takes inverse discrete Fourier transform (IDFT) and inserts cyclic prefix (CP) of length equal to at least the channel memory (L). Pilot tones uniformly inserted in OFDM modulated data for the initial channel estimation [19]. In this work, to simplify the notation, it is assumed that the spreading factor equals to the number of subcarriers and all users have the same spreading factor.

At the receiver, CP is removed and DFT is then applied to the received discrete time signal to obtain the received vector expressed as

$$\mathbf{R} = \mathcal{H}\mathbf{C}\mathbf{b} + \mathbf{W}, \quad (1)$$

where $\mathbf{C} = [\mathbf{c}^1, \dots, \mathbf{c}^K]$ is the $N_c \times K$ spreading code matrix, $\mathbf{b} = [b^1, \dots, b^K]^T$ is the $K \times 1$ vector of the transmitted symbols by the K users. \mathcal{H} is the $N_c \times N_c$ diagonal channel matrix whose elements representing the fading of the subcarriers are modeled in the next section, \mathbf{W} is the $N_c \times 1$ zero-mean, i.i.d. Gaussian vectors that model additive noise in the N_c tones, with variance $\sigma^2/2$ per dimension. Note that due to orthogonality property of the spreading sequences, $\mathbf{C}^T\mathbf{C} = \mathbf{I}_K$.

In this study, our major focus lies on the development of a MAP-EM channel estimation algorithm based on the observation model (1). However, in the sequel we will first present the channel model based on KL expansions.

3. CHANNEL: BASIS EXPANSION MODEL

The fading channel between the transmit and the receive antenna is assumed to be frequency and time selective and the fading process is assumed to be constant during each OFDM symbol. Let $\mathbf{H} = [H_1, H_2, \dots, H_{N_c}]^T$ denote the correlated channel coefficients corresponding to the frequency response of the channel between the transmit and the receive antenna. The KL expansion methodology has been applied for efficient simulation of multipath fading channels [14]. Prompted by the general applicability of KL expansion, we consider in this paper the parameters of \mathbf{H} to be expressed by a linear combination of orthonormal bases,

$$\mathbf{H} = \mathbf{\Psi}\mathbf{G}, \quad (2)$$

where $\mathbf{\Psi} = [c\psi_1, \psi_2, \dots, \psi_{N_c}]$, ψ_i 's are the orthonormal basis vectors, $\mathbf{G} = [G_1, \dots, G_{N_c}]^T$, and G_i is the vector representing the weights of the expansion. By using different basis functions $\mathbf{\Psi}$, we can generate sets of coefficients with different properties. The autocorrelation matrix $\mathbf{C}_H = E[\mathbf{H}\mathbf{H}^\dagger]$ can be decomposed as

$$\mathbf{C}_H = \mathbf{\Psi}\mathbf{\Lambda}\mathbf{\Psi}^\dagger, \quad (3)$$

where $\mathbf{\Lambda} = E\{\mathbf{G}\mathbf{G}^\dagger\}$ is a diagonal. Then (3) represents the *eigendecomposition* of \mathbf{C}_H . The fact that only the eigenvectors diagonalize \mathbf{C}_H leads to the desirable property that the KL coefficients (G_1, \dots, G_{N_c}) are uncorrelated. Furthermore, in the Gaussian case, the uncorrelatedness of the coefficients renders them independent as well, providing additional simplicity. Thus, the channel estimation problem in this study is equivalent to estimating the i.i.d. Gaussian vector \mathbf{G} , namely, the KL expansion coefficients.

4. EM BASED MAP CHANNEL ESTIMATION

In MC-CDMA system, channel equalization is moved from the time domain to the frequency domain, that is, the channel frequency response is estimated. Note that, it is possible to estimate the channel parameters from the time-domain channel model (channel impulse response), in our

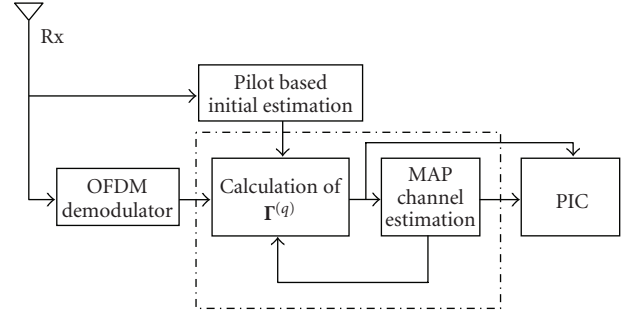


FIGURE 1: Receiver structure for MC-CDMA systems.

work, time-domain approach introduces additional complexity mainly because the frequency domain channel parameters are required and directly employed in the detection process. Moreover, the frequency domain estimator presented in this paper was inspired by the conclusions in [15, 16], where it has been shown that time domain channel estimators based on a Discrete Fourier Transform (DFT) approach for non sample-spaced channels cause aliased spectral leakage and result in an error floor. Furthermore, our proposed frequency domain iterative channel estimation technique employs the KL expansion which reduces the overall computational complexity significantly.

To find MAP estimate of $\hat{\mathbf{G}}$, (1) can be rewritten by using the channel KL expansion as follows:

$$\mathbf{R} = \text{diag}(\mathbf{C}\mathbf{b})\mathbf{\Psi}\mathbf{G} + \mathbf{W}. \quad (4)$$

The MAP estimate $\hat{\mathbf{G}}$ is then given by

$$\hat{\mathbf{G}} = \arg \max_{\mathbf{G}} p(\mathbf{G} | \mathbf{R}) \quad (5)$$

Direct maximization of (5) is mathematically intractable. However, the solution can be obtained easily by means of the iterative EM algorithm. A natural choice for the complete data for this problem is $\chi = \{\mathbf{R}, \mathbf{b}\}$. The vector to be estimated is \mathbf{G} , and the incomplete data is \mathbf{R} . The EM algorithm stated above is equivalent to determining the parameter set \mathbf{G} that maximize the Kullback-Leibler information measure defined by

$$Q(\mathbf{G}|\mathbf{G}^{(q)}) = \sum_b p(\mathbf{R}, \mathbf{b}, \mathbf{G}^{(q)}) \log p(\mathbf{R}, \mathbf{b}, \mathbf{G}), \quad (6)$$

where $\mathbf{G}^{(q)}$ is the estimation of \mathbf{G} at the q th iteration. This algorithm inductively reestimate \mathbf{G} so that a monotonic increase in the *a posteriori* conditional pdf (probability density function) in (5) is guaranteed.

Note that, the term $\log p(\mathbf{R}, \mathbf{b}, \mathbf{G})$ in (6) can be expressed as

$$\log p(\mathbf{R}, \mathbf{b}, \mathbf{G}) = \log p(\mathbf{b} | \mathbf{G}) + \log p(\mathbf{R} | \mathbf{b}, \mathbf{G}) + \log p(\mathbf{G}). \quad (7)$$

The first term on the right-hand side of (7) is constant, since the data sequence \mathbf{b} and \mathbf{G} are independent of each other

and \mathbf{b} have equal *a priori* probability. The probability density function of \mathbf{G} is known *a priori* by the receiver and can be expressed as

$$p(\mathbf{G}) \sim \exp(-\mathbf{G}^\dagger \mathbf{\Lambda}^{-1} \mathbf{G}). \quad (8)$$

Also, given the transmitted symbols \mathbf{b} and the discrete channel representation \mathbf{G} and taking into account the independence of the noise components, the conditional probability density function of the received signal \mathbf{R} can be expressed as

$$p(\mathbf{R} | \mathbf{b}, \mathbf{G}) \sim \exp[-(\mathbf{R} - \text{diag}(\mathbf{C}\mathbf{b})\mathbf{\Psi}\mathbf{G})^\dagger \mathbf{\Sigma}^{-1}(\mathbf{R} - \text{diag}(\mathbf{C}\mathbf{b})\mathbf{\Psi}\mathbf{G})], \quad (9)$$

where $\mathbf{\Sigma}$ is an $N_c \times N_c$ diagonal matrix with $\Sigma[k, k] = \sigma^2$, for $k = 1, 2, \dots, N_c$.

Taking derivatives in (6) with respect to \mathbf{G} and equating the resulting equations to zero, we have

$$\sum_{\mathbf{b}} p(\mathbf{R}, \mathbf{b}, \mathbf{G}^{(q)}) (\mathbf{\Psi}^\dagger \text{diag}(\mathbf{b}^\dagger \mathbf{C}^T) \times \mathbf{\Sigma}^{-1}(\mathbf{R} - \text{diag}(\mathbf{C}\mathbf{b})\mathbf{\Psi}\mathbf{G}) - \mathbf{\Lambda}^{-1} \mathbf{G}) = 0. \quad (10)$$

Note that $p(\mathbf{R}, \mathbf{b}, \mathbf{G}^{(q)})$ may be replaced by $p(\mathbf{b} | \mathbf{R}, \mathbf{G}^{(q)})$ without violating the equalities in (10). Solving (10) for \mathbf{G} , after taking average over \mathbf{b} , the final expression of reestimate of $\hat{\mathbf{G}}^{(q+1)}$ can be obtained as follows:

$$\hat{\mathbf{G}}^{(q+1)} = (\mathbf{T}^{\dagger(q)} \mathbf{T}^{(q)} + \mathbf{\Sigma} \mathbf{\Lambda}^{-1})^{-1} \mathbf{T}^{\dagger(q)} \mathbf{R}, \quad (11)$$

where

$$\mathbf{T}^{(q)} = \text{diag}(\mathbf{C}\mathbf{\Gamma}^{(q)})\mathbf{\Psi}. \quad (12)$$

$\mathbf{\Gamma}^{(q)} = [\Gamma^{(q)}(1), \Gamma^{(q)}(2), \dots, \Gamma^{(q)}(K)]$ represents the *a posteriori probabilities* of the data symbols at the q th iteration step defined as

$$\Gamma^{(q)}(k) = \sum_{b \in S_k} bP(b^k = b | \mathbf{R}, \mathbf{G}^{(q)}). \quad (13)$$

$\mathbf{\Gamma}^{(q)}$ can be computed for QPSK signaling as follows [11]:

$$\mathbf{\Gamma}^{(q)} = \frac{1}{\sqrt{2}} \tanh \left[\frac{\sqrt{2}}{\sigma^2} \text{Re}(\hat{\mathbf{Z}}^{(q)}) \right] + \frac{j}{\sqrt{2}} \tanh \left[\frac{\sqrt{2}}{\sigma^2} \text{Im}(\hat{\mathbf{Z}}^{(q)}) \right], \quad (14)$$

where

$$\hat{\mathbf{Z}}^{(q)} = \mathbf{C}^T (\hat{\mathcal{H}}^{\dagger(q)} \hat{\mathcal{H}}^{(q)} + \sigma^2 \mathbf{I}_{N_c})^{-1} \hat{\mathcal{H}}^{\dagger(q)} \mathbf{R}. \quad (15)$$

Finally, the data \mathbf{b} transmitted by each user can be estimated at the q th iteration step as

$$\hat{\mathbf{b}}^{(q)} = \frac{1}{\sqrt{2}} \text{csign}(\mathbf{\Gamma}^{(q)}), \quad (16)$$

where “csign” is defined as $\text{csign}(a + jb) = \text{sign}(a) + j\text{sign}(b)$.

Truncation property

A truncated expansion vector \mathbf{G}_r be formed from \mathbf{G} by selecting r orthonormal basis vectors among all basis vectors that satisfy $\mathbf{C}_H \mathbf{\Psi} = \mathbf{\Psi} \mathbf{\Lambda}$. The optimal solution that yields the smallest average mean-squared truncation error $(1/N_c) E[\boldsymbol{\epsilon}_r^\dagger \boldsymbol{\epsilon}_r]$ is the one expanded with the orthonormal basis vectors associated with the first largest r eigenvalues as given by

$$\frac{1}{N_c - r} E[\boldsymbol{\epsilon}_r^\dagger \boldsymbol{\epsilon}_r] = \frac{1}{N_c - r} \sum_{i=r}^{N_c} \lambda_i, \quad (17)$$

where $\boldsymbol{\epsilon}_r = \mathbf{G} - \mathbf{G}_r$. For the problem at hand, truncation property of the KL expansion results in a low-rank approximation as well. Thus, a rank- r approximation of $\mathbf{\Lambda}$ can be defined as $\mathbf{\Lambda}_r = \text{diag}\{\lambda_1, \lambda_2, \dots, \lambda_r\}$ by ignoring the trailing $N_c - r$ variances $\{\lambda_i\}_{i=r}^{N_c}$, since they are very small compared to the leading r variances $\{\lambda_i\}_{i=1}^r$. Actually, the pattern of eigenvalues for $\mathbf{\Lambda}$ typically splits the eigenvectors into dominant and subdominant sets. Then the choice of r is more or less obvious. For instance, if the number of parameters in the expansion include dominant eigenvalues, it is possible to obtain a good approximation with a relatively small number of KL coefficients.

Complexity

Based on the approach presented in [17], the traditional LMMSE estimation for \mathbf{H} can be easily expressed as

$$\hat{\mathbf{H}} = \underbrace{\mathbf{C}_H [\mathbf{C}_H + \mathbf{\Sigma} (\text{diag}(\mathbf{C}\mathbf{b}) \text{diag}(\mathbf{C}\mathbf{b}))^{-1}]^{-1}}_{\text{“}O(N_c^3)\text{” computational complexity}} \times [\text{diag}(\mathbf{C}\mathbf{b})]^{-1} \mathbf{R}. \quad (18)$$

Since $[\mathbf{C}_H + \mathbf{\Sigma} (\text{diag}(\mathbf{C}\mathbf{b}) \text{diag}(\mathbf{C}\mathbf{b}))^{-1}]^{-1}$ changes with data symbols, its inverse cannot be precomputed and has high computational complexity due to required large-scale matrix inversion.¹ Moreover, the error caused by the small fluctuations in \mathbf{C}_H and $\mathbf{\Sigma}$ have an amplified effect on the channel estimation due to the matrix inversion. Furthermore, this effect becomes more severe as the dimension of the matrix, to be inverted, increases [18]. Therefore, the KL-based approach is needed to avoid large-scale matrix inversion. Using (2) and (11), the iterative estimate of \mathbf{H} with KL expansion can be obtained as

$$\hat{\mathbf{H}}^{(q+1)} = \mathbf{\Psi} (\mathbf{T}^{\dagger(q)} \mathbf{T}^{(q)} + \mathbf{\Sigma} \mathbf{\Lambda}^{-1})^{-1} \mathbf{T}^{\dagger(q)} \mathbf{R}. \quad (19)$$

However, in this form, complexity of channel estimate is greater than the traditional LMMSE estimate. Therefore, to reduce the complexity of the estimator further we rewrite (19) as

$$\hat{\mathbf{H}}^{(q+1)} = \mathbf{\Psi} \mathbf{\Lambda} (\mathbf{\Lambda} \mathbf{T}^{\dagger(q)} \mathbf{T}^{(q)} \mathbf{\Lambda} + \mathbf{\Sigma} \mathbf{\Lambda})^{-1} \mathbf{\Lambda} \mathbf{T}^{\dagger(q)} \mathbf{R} \quad (20)$$

¹ The computational complexity of an $N_c \times N_c$ matrix inversion, using Gaussian elimination is $O(N_c^3)$.

TABLE 1

Algorithm	Computational complexity
LMMSE	$2N_c^2 + 5N_c + N_c K + O(N_c^3)$
KL	$N_c^3 + 4N_c^2 + N_c K + 2N_c + O(N_c^3)$
KL-truncated	$N_c r^2 + 3N_c r + r^2 + N_c K + 2r + O(r^3)$

and proceed with the low-rank approximations by considering only r column vectors of $\mathbf{\Psi}$ and \mathbf{T} corresponding to the r largest eigenvalues of $\mathbf{\Lambda}$, yielding

$$\hat{\mathbf{H}}^{(q+1)} = \mathbf{\Psi}_r \mathbf{\Lambda}_r \underbrace{(\mathbf{\Lambda}_r \mathbf{T}_r^{(q)} \mathbf{T}_r^{(q)} \mathbf{\Lambda}_r + \mathbf{\Sigma}_r \mathbf{\Lambda}_r)^{-1}}_{\text{"O}(r^3)" \text{ computational complexity}} \mathbf{\Lambda}_r \mathbf{T}_r^{(q)} \mathbf{R}, \quad (21)$$

where $\mathbf{\Sigma}_r$ is an $r \times r$ diagonal matrix whose elements are equal to σ^2 . $\mathbf{\Psi}_r$ and \mathbf{T}_r are in (21) an $N_c \times r$ matrices which can be formed by omitting the last $N_c - r$ columns of $\mathbf{\Psi}$ and \mathbf{T} , respectively. Equation (21) can then be rearranged as follows:

$$\hat{\mathbf{H}}^{(q+1)} = \mathbf{\Psi}_r (\mathbf{T}_r^{(q)} \mathbf{T}_r^{(q)} + \mathbf{\Sigma}_r \mathbf{\Lambda}_r^{-1})^{-1} \mathbf{T}_r^{(q)} \mathbf{R}. \quad (22)$$

Thus, the low-rank expansion yields an excellent approximation with a relatively small number of KL coefficients. Computational complexity has been evaluated quantitatively and summarized in Table 1.

5. PARALLEL INTERFACE CANCELLATION (PIC)

The estimated complex QPSK vector $\hat{\mathbf{b}}$ given by (16) is passed to a PIC module after last iteration. In this module, the calculation of all interfering signals for user k can be written as

$$\mathbf{R}_{\text{int}}^k = \hat{\mathcal{H}} \mathbf{C} \hat{\mathbf{b}} \quad \text{for } \hat{b}^k = 0. \quad (23)$$

Interfering signals for user k subtracted from the received signal \mathbf{R} , then passed to the single user detector. Finally, the PIC detector for k th user can be written as

$$b_{\text{pic}}^k = (\mathbf{c}^k)^T [\hat{\mathcal{H}} (\mathbf{R} - \mathbf{R}_{\text{int}}^k)] \quad \text{for } k = 1, \dots, K. \quad (24)$$

For the last iteration, detected symbols for QPSK modulation are

$$\hat{b}_{\text{pic}}^k = \frac{1}{\sqrt{2}} \text{csign}(b_{\text{pic}}^k) \quad \text{for } k = 1, \dots, K. \quad (25)$$

Initialization

Given the received signal \mathbf{R} , the EM algorithm starts with an initial value $\mathbf{G}^{(0)}$ of the unknown channel parameters \mathbf{G} . Corresponding to pilot symbols, we focus on a under-sampled signal model and employ the linear minimum mean-square error (LMMSE) estimate to obtain the under-sampled channel parameters. Then the complete initial channel gains can easily be determined using an interpolation technique, that is, Lagrange interpolation algorithm. Finally, the initial values of $\mathbf{G}_\mu^{(0)}$ are used in the iterative EM algorithm to avoid divergence. The details of the initialization process are presented in [11, 17].

6. MODIFIED CRAMER-RAO BOUND

The modified Fisher information matrix (FIM) can be obtained by a straightforward modification of FIM as [11],

$$\mathbf{J}_M(\mathbf{G}) \triangleq \underbrace{-E \left[\frac{\partial^2 \ln p(\mathbf{R} | \mathbf{G})}{\partial \mathbf{G}^* \partial \mathbf{G}^T} \right]}_{\mathbf{J}(\mathbf{G})} - \underbrace{E \left[\frac{\partial^2 \ln p(\mathbf{G})}{\partial \mathbf{G}^* \partial \mathbf{G}^T} \right]}_{\mathbf{J}_p(\mathbf{G})}, \quad (26)$$

where $\mathbf{J}_p(\mathbf{G})$ represents the *a priori* information.

Under the assumption that \mathbf{G} and \mathbf{W} are independent of each other and \mathbf{W} is a zero-mean Gaussian vector, the transmitted signals become uncorrelated due to the orthogonal spreading codes. The conditional PDF of \mathbf{R} given \mathbf{G} can be obtained by averaging $p(\mathbf{R} | \mathbf{b}, \mathbf{G})$ over \mathbf{b} as follows

$$p(\mathbf{R} | \mathbf{G}) = E_{\mathbf{b}} \{ p(\mathbf{R} | \mathbf{b}, \mathbf{G}) \}. \quad (27)$$

From (27), the derivatives can be taken as follows:

$$\begin{aligned} \frac{\partial \ln p(\mathbf{R} | \mathbf{G})}{\partial \mathbf{G}^T} &= \frac{1}{\sigma^2} (\mathbf{R} - \text{diag}(\mathbf{C} \mathbf{b}) \mathbf{\Psi} \mathbf{G})^\dagger \text{diag}(\mathbf{C} \mathbf{b}) \mathbf{\Psi}, \\ \frac{\partial^2 \ln p(\tilde{\mathbf{R}} | \mathbf{G})}{\partial \mathbf{G}^* \partial \mathbf{G}^T} &= -\frac{1}{\sigma^2} \tilde{\mathbf{\Psi}}^\dagger \text{diag}(\mathbf{b}^T \mathbf{C}^T) \text{diag}(\mathbf{C} \mathbf{b}) \tilde{\mathbf{\Psi}}. \end{aligned} \quad (28)$$

Second term in (26) is easily obtained as follows:

$$\frac{\partial \ln p(\mathbf{G})}{\partial \mathbf{G}^T} = -\mathbf{G}^\dagger \mathbf{\Lambda}^{-1}, \quad \frac{\partial^2 \ln p(\mathbf{G})}{\partial \mathbf{G}^* \partial \mathbf{G}^T} = -\mathbf{\Lambda}^{-1}. \quad (29)$$

Taking the negative expectations, the first and the second term in (26) becomes $\mathbf{J}(\mathbf{G}) = (1/\sigma^2) \mathbf{I}_{N_c}$ and $\mathbf{J}_p(\mathbf{G}) = \mathbf{\Lambda}^{-1}$, respectively. Finally, (26) produces for the modified FIM as follows:

$$\mathbf{J}_M(\mathbf{G}) = \frac{1}{\sigma^2} \mathbf{I}_{N_c} + \mathbf{\Lambda}^{-1}. \quad (30)$$

Inverting the matrix $\mathbf{J}_M(\mathbf{G})$ yields $\text{MCRB}(\hat{\mathbf{G}}) = \mathbf{J}_M^{-1}(\mathbf{G})$. $\text{MCRB}(\hat{\mathbf{G}})$ is a diagonal matrix with the elements on the main diagonal equaling the reciprocal of those $\mathbf{J}(\mathbf{G})$ matrices.

7. SIMULATIONS

In this section, performance of the MC-CDMA system based on the proposed receivers is investigated by computer simulations operating over frequency selective channels. In simulation, we assume that all users receive the same power. The orthogonal Gold sequence code is selected as spreading code and the processing gain equals to the number of subcarriers. The assumption of a full-load system is made throughout the simulations except Figure 4, that is the number of active users K , is equal to the length of the spreading code $N_c = 128$.

The correlative channel coefficients, \mathbf{H} , have exponentially decaying power delay profiles, described by $\theta(\tau_\mu) = C \exp(-\tau_\mu/\tau_{\text{rms}})$. The delays τ_μ are uniformly and independently distributed over the length of the cyclic prefix. τ_{rms} determines the decay of the power-delay profile and C is

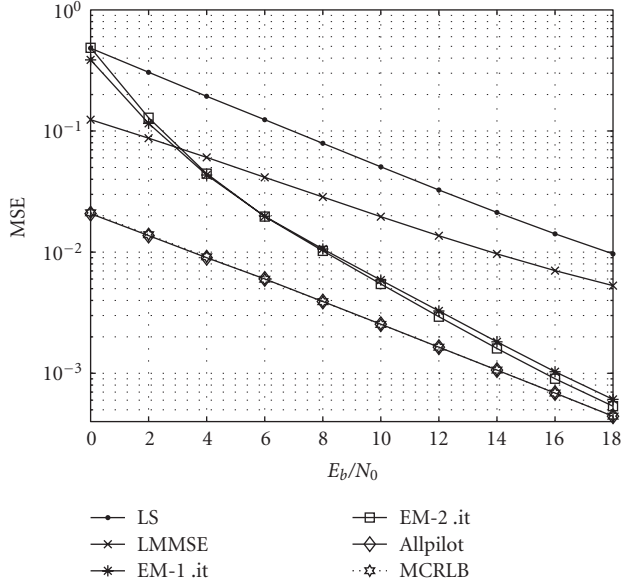


FIGURE 2: Comparison of different channel estimation algorithms (MSE).

the normalizing constant. Note that the normalized discrete channel-correlations for different subcarriers and blocks of this channel model were presented in [17] as follows:

$$C_H(k, k') = \frac{1 - \exp[-L(1/\tau_{\text{rms}} + 2\pi j(k - k')/N_c)]}{\tau_{\text{rms}}(1 - \exp(-L/\tau_{\text{rms}}))(1/\tau_{\text{rms}} + j2\pi(k - k')/N_c)} \quad (31)$$

where (k, k') denotes different subcarriers, L is the cyclic prefix, N_c is the total number of subcarriers. The system has an 800 KHz bandwidth and is divided into $N_c = 128$ tones with a total period T_s of 165 microseconds, of which 5 microseconds constitute the cyclic prefix ($L = 4$). We assume that the rms value of the multipath width is $\tau_{\text{rms}} = 1$ sample (1.25 microseconds) for the power-delay profile. With the τ_{rms} value chosen and to avoid ISI, the guard interval duration is chosen to be equal to 4 sample (5 microseconds)[17].

7.1. Performance evaluation

The performance merits of the proposed structure over other candidates are confirmed by corroborating simulations. Figure 2 compares the MSE performance of the EM-MAP channel estimation approach with a widely used LS and LMMSE pilot symbol assisted modulation (PSAM) schemes [14], as well as all-pilot estimation for MC-CDMA systems. Pilot insertion rate (PIR) was chosen as PIR = 1 : 8 That is one pilot is inserted for every 8 data symbols. It is observed that the proposed EM-MAP significantly outperforms the LS as well as LMMSE techniques and approaches the all-pilot estimation case and the MCRLB at higher E_b/N_0 values. Moreover, the BER performance of the proposed system is also studied for different detection schemes in Figure 3. It is

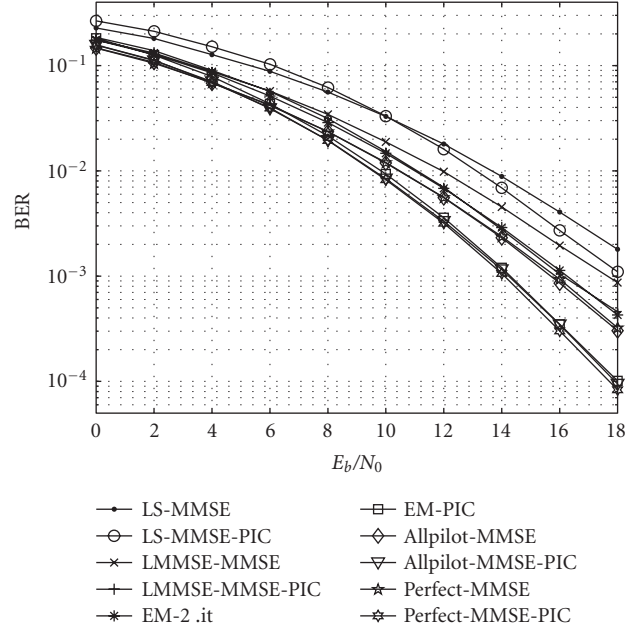


FIGURE 3: BER performances of receiver structures for full load system.

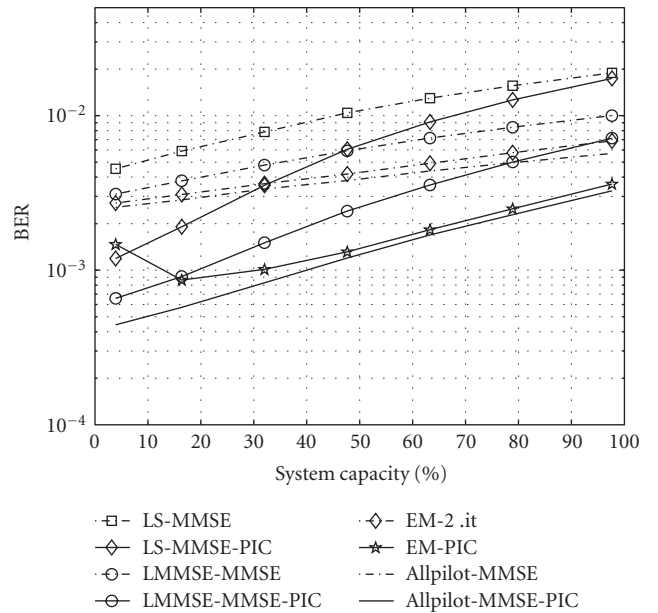


FIGURE 4: BER performances of receiver structures in terms of system capacity usage.

shown that the BER performance of the proposed receiver structure is much better than the combined MMSE-PIC receiver in the case of LS, LMMSE while approaches the performance of the all-pilot and perfect channel estimation cases.

We also determined BER performance of the algorithm as a function of the system capacity usage for $E_b/N_0 = 12$ dB. As shown in Figure 4, the BER performance will degrade as the total capacity usage approaches full load for both two detection schemes. On the other hand, our simulation results

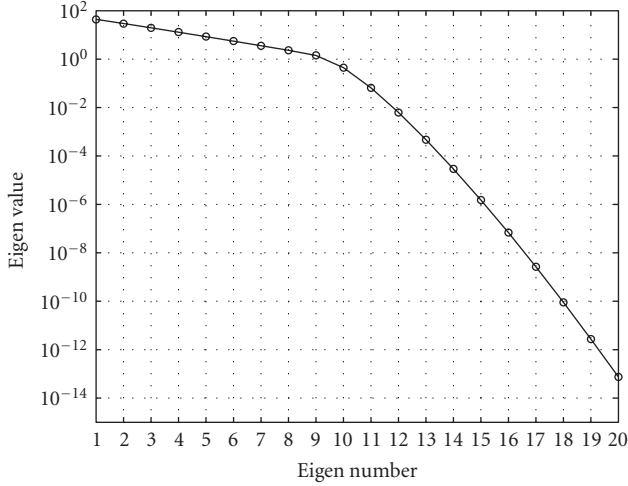


FIGURE 5: Eigenvalue spectrum.

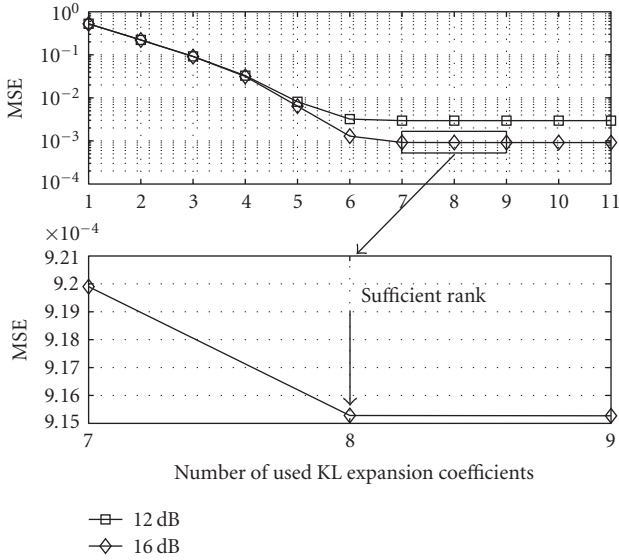


FIGURE 6: Optimal truncation property of the KL expansion.

show that the performance difference between MMSE and MMSE-PIC detection becomes more distinguishable as the total active users decreases.

7.2. The optimal truncation property

The KL expansion minimizes the amount of information required to represent the statistically dependent data. Thus, this property can further reduce the computational load of the channel estimation algorithm. An example of the Eigenspectrum is shown in Figure 5 for the correlation matrix of the channel given in (31). Since the Eigenspectrum of the correlation matrix among different frequencies has an exponential profile, a reduced set of channel parameters can be employed. Therefore, the optimal truncation property of the KL expansion is exploited in Figure 6 where MSE performances versus the number of coefficient used KL expansion

are given for 12 dB and 16 dB. If the number of parameters in the expansion includes dominant eigenvalues (Rank = 8), it is possible to obtain an excellent approximation with a relatively small number of KL coefficients.

7.3. Mismatch simulations

Once the true frequency-domain correlation, characterizing the channel statistics and the SNR values, is known, the channel estimator can be designed as indicated in Section 4. In the previous simulations, the autocorrelation matrix and the SNR were assumed to be available as *a priori* information at the receiver. However, in practice the true channel correlation and the SNR are not known. It is then important to analyze the performance degradation due to a mismatch of the estimator to the channel statistics to check its robustness to the variation of these parameters.

Correlation mismatch

We designed the estimator for a uniform channel correlation which gives the worst MSE performance among all channel models and evaluated it for an exponentially decaying power delay profile. Note that as τ_{rms} goes to infinity, the power delay profile of the channel given by (31) approaches to the uniform power delay profile with autocorrelation

$$\tilde{C}_H(k, k') = \begin{cases} 1 & \text{if } k = k' \\ \frac{1 - e^{-j2\pi L(k-k')/N_c}}{2\pi jL(k-k')/N_c} & \text{if } k \neq k'. \end{cases} \quad (32)$$

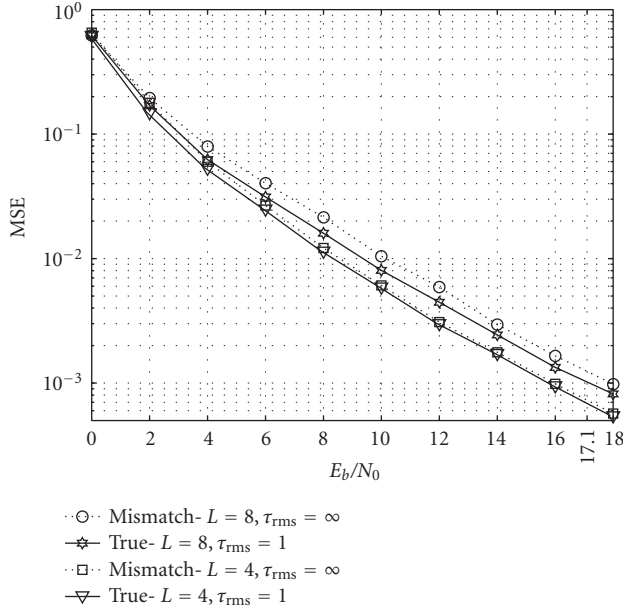
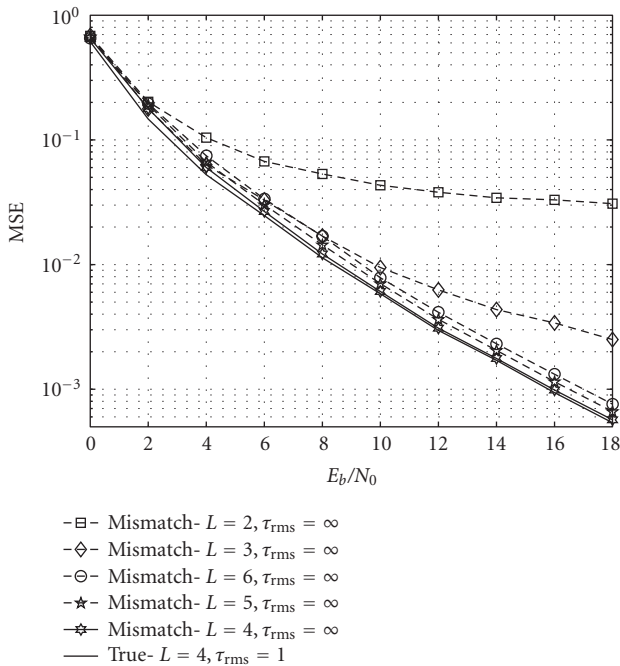
Figure 7 demonstrates the estimator’s sensitivity to the channel statistics as a function of the average MSE performance for the following mismatch cases.

Case 1. True statistic $\Rightarrow \tau_{rms} = 1, L = 4, N_c = 128$.
Mismatch $\Rightarrow \tau_{rms} = \infty, L = 4, N_c = 128$.

Case 2. True statistic $\Rightarrow \tau_{rms} = 1, L = 8, N_c = 128$.
Mismatch $\Rightarrow \tau_{rms} = \infty, L = 8, N_c = 128$.

From the mismatch curves presented in Figure 7, it is seen that for Case 1, practically there is no mismatch degradation observed when the estimator is designed for mismatched channel statistics specified above. Thus, we conclude that the estimator is quite robust against the channel correlation mismatch for Case 1. For Case 2 frequency selectivity of the channel is increased by increasing the channel length L . In this case, we observed that the mismatch performance of the estimator was degraded moderately. In fact, the performance degradation between true and mismatch cases is approximately 0.9 dB for BER = 10^{-3} .

In Figure 8, we investigate again sensitivity of estimator to the channel statistics between the true correlation with $\tau_{rms} = 1$ and the effective channel length $L = 4$ against $\tau_{rms} = \infty$ and for $L = 2, 3, 4, 5, 6$. We conclude from the mismatch curves presented in Figure 8 that the mismatch affects substantially on the MSE performance when L is less than the correct channel length, and affects less when L is greater than the correct channel length.

FIGURE 7: Correlation mismatch for τ_{rms} .FIGURE 8: Correlation mismatch for L and τ_{rms} .

SNR mismatch

The BER curves for a design SNR of 5 dB, 10 dB, and 15 dB are shown in Figure 9 with the true SNR performance. The performance of the EM-MAP estimator for high SNR (15 dB) design is better than low-SNR (5 dB) design across a range of SNR values (10–18 dB). These results confirm that the channel estimation error is concealed in noise for low SNR whereas it tends to dominate for high SNR. Thus, the system performance degrades especially at low-SNR region.

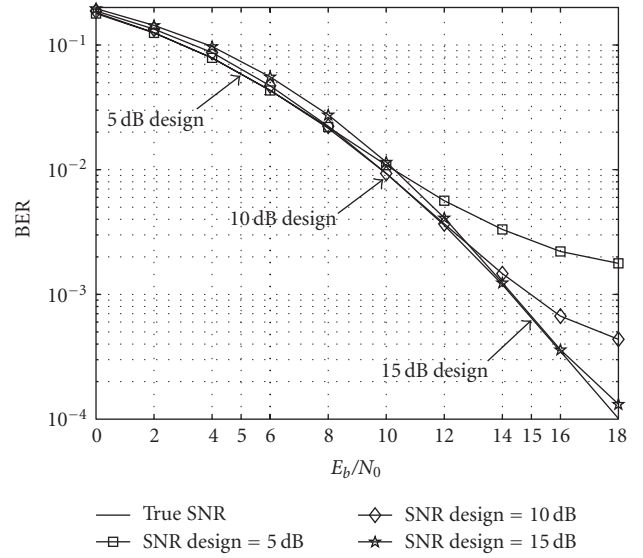


FIGURE 9: SNR mismatch.

8. CONCLUSIONS

In this work we have presented an efficient EM-MAP channel-estimation-based PIC receiver structure for downlink MC-CDMA systems. This algorithm performs an iterative estimation of the channel according to the MAP criterion, using the EM algorithm employing MPSK modulation scheme with additive Gaussian noise. Furthermore, the advantage of this algorithm, besides its simple implementation, is that the channel estimation is instantaneous, since the signal and the pilot are orthogonal code division multiplexed (OCDM) and they are distorted at the same time. Moreover, it was shown that KL expansion without optimal truncation property did not enable us to estimate the channel in a very simple way without taking inverse of large dimensional matrices for MC-CDMA systems. Computer simulation results have indicated that the MSE and BER performance of the proposed algorithm is well over the conventional algorithms and approaches to the MCRLB by iterative improvement. Finally, we have also investigated the effect of modelling mismatch on the estimator performance. It was concluded that the performance degradation due to such mismatch is negligible especially at low SNR values.

ACKNOWLEDGMENTS

This work was supported in part by the Turkish Scientific and Technical Research Institute (TUBITAK) under Grant no. 104E166 and the Research Fund of Istanbul University under Projects UDP-889/22122006, UDP- 921/09052007, T-856/02062006. This research has been also conducted within the NEWCOM++ Network of Excellence in Wireless Communications funded through the EC 7th Framework Programme. Part of the results of this paper was presented at the IEEE Wireless Communications and Networking Conference (WCNC-2007), March 11–15 2007, Hong Kong.

REFERENCES

- [1] N. Yee, J.-P. Linnarz, and G. Fettweis, "Multi-carrier CDMA in indoor wireless radio networks," in *Proceedings of the 4th IEEE International Symposium on Personal, Indoor and Mobile Radio Communications (PIMRC '93)*, pp. 109–113, Yokohama, Japan, September 1993.
- [2] K. Fazel and L. Papke, "On the performance of convolutionally-coded CDMA/OFDM for mobile communication system," in *Proceedings of the 4th IEEE International Symposium on Personal, Indoor and Mobile Radio Communications (PIMRC '93)*, pp. 468–472, Yokohama, Japan, September 1993.
- [3] S. Hara and R. Prasad, "Overview of multicarrier CDMA," *IEEE Communications Magazine*, vol. 35, no. 12, pp. 126–133, 1997.
- [4] S. Iraj, T. Sipila, and J. Lilleberg, "Channel estimation and signal detection for MC-CDMA in multipath fading channels," in *Proceedings of the 4th IEEE International Symposium on Personal, Indoor and Mobile Radio Communications (PIMRC '93)*, Yokohama, Japan, September 1993.
- [5] V. Kuhn, "Combined MMSE-PIC in coded OFDM-CDMA systems," in *Proceedings of the IEEE Global Conference on Telecommunications (Globecom '01)*, pp. 231–235, San Antonio, Tex, USA, November 2001.
- [6] M. Feder and E. Weinstein, "Parameter Estimation of superimposed signals using the EM algorithm," *IEEE Transactions on Acoustics, Speech, and Signal Processing*, vol. 36, no. 4, pp. 477–489, 1988.
- [7] Y. Xie and C. N. Georghiades, "Two EM-type channel estimation algorithms for OFDM with transmitter diversity," *IEEE Transactions on Communications*, vol. 51, no. 1, pp. 106–115, 2003.
- [8] L. B. Nelson and H. V. Poor, "Iterative multiuser receivers for CDMA channels: an EM-based approach," *IEEE Transactions on Communications*, vol. 44, no. 12, pp. 1700–1710, 1996.
- [9] A. Kocian and B. H. Fleury, "EM-based joint data detection and channel estimation of DS-SS signals," *IEEE Transactions on Communications*, vol. 51, no. 10, pp. 1709–1720, 2003.
- [10] A. A. D'Amico, U. Mengali, and M. Morelli, "Channel estimation for the uplink of a DS-SS system," *IEEE Transactions on Wireless Communications*, vol. 2, no. 6, pp. 1132–1137, 2003.
- [11] H. A. Çirpan, E. Panayirci, and H. Dogan, "Nondata-aided channel estimation for OFDM systems with space-frequency transmit diversity," *IEEE Transactions on Vehicular Technology*, vol. 55, no. 2, pp. 449–457, 2006.
- [12] H. Dogan, H. A. Çirpan, and E. Panayirci, "Iterative channel estimation and decoding of turbo coded SFBC-OFDM systems," *IEEE Transactions on Wireless Communications*, vol. 6, no. 8, pp. 3090–3101, 2007.
- [13] S. M. Kay, *Fundamentals of Statistical Signal Processing: Estimation Theory*, Prentice-Hall, Englewood Cliffs, NJ, USA, 1993.
- [14] K. W. Yip and T.-S. Ng, "Karhunen-Loeve expansion of the WSSUS channel output and its application to efficient simulation," *IEEE Journal on Selected Areas in Communications*, vol. 15, no. 4, pp. 640–646, 1997.
- [15] B. Yang, Z. Cao, and K. B. Letaief, "Analysis of low-complexity windowed DFT-based MMSE channel estimator for OFDM systems," *IEEE Transactions on Communications*, vol. 49, no. 11, pp. 1977–1987, 2001.
- [16] O. Edfors, M. Sandell, J. J. van de Beek, S. K. Wilson, and P. O. Borjesson, "Analysis of DFT-based channel estimation for OFDM," *Wireless Personal Communications*, vol. 12, no. 1, pp. 55–70, 2000.
- [17] O. Edfors, M. Sandell, J.-J. van de Beek, S. K. Wilson, and P. O. Borjesson, "OFDM channel estimation by singular value decomposition," *IEEE Transactions on Communications*, vol. 46, no. 7, pp. 931–936, 1998.
- [18] J. Zhu and W. Lee, "A low-complexity channel estimator for OFDM systems in multipath fading channels," in *Proceedings of 15th IEEE International Symposium on Personal, Indoor and Mobile Radio Communications (PIMRC '04)*, vol. 3, pp. 1978–1982, Barcelona, Spain, September 2004.
- [19] S. Coleri, M. Ergen, A. Puri, and A. Bahai, "Channel estimation techniques based on pilot arrangement in OFDM systems," *IEEE Transactions on Broadcasting*, vol. 48, no. 3, pp. 223–229, 2002.